



Differences in Brain Morphology between Hydrocephalus Ex Vacuo and Idiopathic Normal Pressure Hydrocephalus

Minkyung Kim^{1*}, Sun-Won Park^{2,3*}, Jun-Young Lee⁴ ✉, Hongrae Kim⁴, Jung Hyo Rhim², Soowon Park⁵, Jee-Young Lee⁶, Hwancheol Son⁷, Yu Kyeong Kim⁸, and Sang Hyung Lee⁹ ✉

¹Seoul National University College of Medicine, Seoul, Republic of Korea

²Department of Radiology, SMG-SNU Boramae Medical Center, Seoul, Republic of Korea

³Department of Radiology, Seoul National University College of Medicine, Seoul, Republic of Korea

⁴Department of Psychiatry, Seoul National University College of Medicine & SMG-SNU Boramae Medical Center, Seoul, Republic of Korea

⁵Department of Teacher Education, College of Liberal Arts and Interdisciplinary Studies, Kyonggi University, Suwon, Republic of Korea

⁶Department of Neurology, SMG-SNU Boramae Medical Center, Seoul, Republic of Korea

⁷Department of Urology, Seoul National University College of Medicine & SMG-SNU Boramae Medical Center, Seoul, Republic of Korea

⁸Department of Nuclear Medicine, SMG-SNU Boramae Medical Center, Seoul, Republic of Korea

⁹Department of Neurosurgery, Seoul National University College of Medicine & SMG-SNU Boramae Medical Center, Seoul, Republic of Korea

Objective The distinction between idiopathic normal pressure hydrocephalus (iNPH) and hydrocephalus ex vacuo caused by encephalic volume loss remains to be established. This study aims to investigate radiological parameters as clinically useful tools to discriminate iNPH from hydrocephalus ex vacuo caused by Alzheimer's disease (AD).

Methods A total of 54 patients with ventriculomegaly (iNPH, 25; hydrocephalus ex vacuo, 29) were recruited in this study. Consequently, nine radiological parameters were compared between iNPH and hydrocephalus ex vacuo using magnetic resonance imaging (MRI).

Results A small callosal angle (CA), the Sylvian fissure dilatation, and absence of narrowing of superior parietal sulci discriminated the iNPH group from the hydrocephalus ex vacuo group ($p < 0.05$). The final binary logistic regression model included narrowing of superior parietal sulci, degrees of the CA, and height of the Sylvian fissure after controlling for age and global Clinical Dementia Rating (CDR). The composite score made from these three indicators (narrowing of superior parietal sulci, degrees of the CA, and height of the Sylvian fissure) was statistically different between iNPH and hydrocephalus ex vacuo.

Conclusion The narrowing of the CA, dilatation of the Sylvian fissure, and narrowing of superior parietal sulci may be used as radiological key indices and noninvasive tools for the differential diagnosis of iNPH from hydrocephalus ex vacuo.

Psychiatry Investig 2021;18(7):628-635

Key Words Normal pressure hydrocephalus, Dementia, Hydrocephalus ex vacuo, Alzheimer's disease, Magnetic resonance imaging.

INTRODUCTION

Alzheimer's disease (AD) which causes cognitive decline often demonstrates moderate to severe ventriculomegaly. This pathology is called, known as hydrocephalus ex vacuo, a com-

pensatory enlargement of the cerebrospinal fluid (CSF) spaces caused by degenerative encephalic volume loss. Idiopathic normal pressure hydrocephalus (iNPH) typically manifests during adult life as an insidiously progressive, chronic disorder that lacks an identifiable antecedent cause.¹ It is characterized by

Received: September 17, 2020 **Revised:** December 30, 2020 **Accepted:** April 10, 2021

✉ **Correspondence:** Jun-Young Lee, MD, PhD

Department of Psychiatry, Seoul National University College of Medicine & SMG-SNU Boramae Medical Center, 20 Boramae-ro 5-gil, Dongjak-gu, Seoul 07061, Republic of Korea

Tel: +82-2-870-2581, **Fax:** +82-2-870-2587, **E-mail:** benji@snu.ac.kr

✉ **Correspondence:** Sang Hyung Lee, MD, PhD

Department of Neurosurgery, Seoul National University College of Medicine & SMG-SNU Boramae Medical Center, 20 Boramae-ro 5-gil, Dongjak-gu, Seoul 07061, Republic of Korea

Tel: +82-2-870-2302, **Fax:** +82-2-870-3864, **E-mail:** nslee@snu.ac.kr

*These authors contributed equally to this work.

Portions of this paper were presented in poster form at the Alzheimer's Association International Conference in Los Angeles, USA, on July 14–17, 2019.

© This is an Open Access article distributed under the terms of the Creative Commons Attribution Non-Commercial License (<https://creativecommons.org/licenses/by-nc/4.0>) which permits unrestricted non-commercial use, distribution, and reproduction in any medium, provided the original work is properly cited.

ventricular enlargement in the setting of normal intracranial pressure with no visible obstruction to CSF flow. Additionally, there can be other various imaging findings such as enlargement of the temporal horns of the lateral ventricles, callosal angle of 40 degree or more, evidence of altered brain water content, and an aqueductal or fourth ventricular flow void on MRI. Clinically, gait and/or balance impairments are usual symptoms, and findings may also include disturbances in cognition and control of urination. This condition represents an increasingly significant health issue due to steadily growing survival age of the population within the developed countries.²

It often presents cognitive impairment similar to AD, due usually to a gradual block of the drainage of CSF in the brain. The proper differential diagnosis for iNPH holds clinical significance because shunt therapy can improve its clinical symptoms unlike those of AD.³ Furthermore, a recent normal pressure hydrocephalus (NPH) study suggested that the presence of AD pathology predicts poor prognosis after shunt therapy, accentuating the imperative clinical value for an accurate differential diagnosis between AD and iNPH.⁴ Although the CSF tap test is an invasive procedure and lacks sensitivity (0.26–0.61) for diagnosing iNPH, it is effective in predicting shunt response for patients with ventriculomegaly.⁵ Therefore, researches have focused on improving diagnosis through noninvasive imaging techniques between these two diseases. Since it is reported that similar to AD, the prevalence of NPH increases with age,⁶ distinguishing noninvasively iNPH from hydrocephalus ex vacuo becomes very important and is a challenging task.

Existing studies have largely focused on differentiating patients with iNPH from healthy controls, but more researches are being published to compare with patients with AD with already advanced ventriculomegaly.^{7,8} Parameters such as the degree of the callosal angle (CA), width of the temporal horn, and the Evans' index (EI) have been presented to differentiate the brain imaging of iNPH from AD. However, these tools are controversial and require more integrated research through a variety of brain imaging indicators.^{9,10} Different studies reported varying diagnostic sensitivities and specificities of radiological parameters and even controversial results concerning the most commonly used radiological markers such as Evans' Index (EI) or callosal angle (CA).^{11,12} Thus, finding out more accurate and reflectable brain imaging parameters to distinguish between iNPH and AD is necessary. Consequently, this study used brain magnetic resonance imaging (MRI) to identify the neuroradiological distinctions between iNPH and hydrocephalus ex vacuo through the following nine neuroimaging parameters, which have been commonly used in the study of radiological parameters comparing iNPH with AD: EI, degrees of the CA, narrowing of the superior parietal sulci, height of the Sylvian fissure, width of the temporal horn, dilation of the perihippocampal

fissure (PHF), presence of focally enlarged cerebral sulci, severity of periventricular hyperintensities, and medial temporal lobe atrophy scale. In addition, the usefulness of these combined parameters in distinguishing iNPH from AD than each element was looked into.

METHODS

Participants

Overall, 77 patients diagnosed with ventriculomegaly at SMG-SNU Boramae Medical Center from January 2013 to December 2018 detected by MRI using an Evans' ratio of at least 0.3 were retrospectively recruited in this study. The Evans' ratio is defined as the maximum ventricular width divided by the largest frontal distance between the inner tables of the skull. Patients >85 and <55 years old, history of head injury, brain tumor or cerebral infarction/hemorrhage, drug and alcohol abuse, and Parkinson's disease were the exclusion criteria. Of the 77 selected patients, 29 patients with probable AD were diagnosed based on the National Institute of Neurological and Communicative Diseases and Stroke/Alzheimer's Disease and Related Disorders Association criteria.¹³ Moreover, 25 patients with probable iNPH were identified based on the 2005 iNPH International Criteria and the updated references based on these criteria.¹ Probable iNPH would typically have gait disturbance plus at least one other area of impairment in cognition, urinary symptoms, or both, and ventriculomegaly seen on brain imaging. There were 23 subjects that could not be distinguished between the two diseases; they were excluded from the study.

Standard protocol approvals, registrations, and patient consents

This study was performed following the ethical standards established in the 1964 Declaration of Helsinki and was approved by the Ethics Board of SMG-SNU Boramae Medical Center (IRB No. 26-2014-42). All subjects or responsible caregivers were waived from their informed consent by the IRB of SMG-SNU Medical Center since this study was performed retrospectively.

MRI analysis

In 54 patients (25 patients with iNPH and 29 patients with AD), T1-weighted coronal MRI images were attained through the 3.0-Tesla MRI scanner (Philips, Achieva, Harvey, IL, USA) based on the following radiological parameters: repetition time (9.9 ms), echo time (4.6 ms), flip angle (8°), field of view (220 mm), matrix size (220×220 pixels), and slice thickness (1 mm). The axial T2-weighted fluid-attenuated inversion recovery images were also attained. Two neuroradiologists rated each patient's image without prior insight on the patient's

medical information. The radiologists reached a final decision after a consensus meeting in case of discrepancies. Figure 1 shows the following radiological parameters evaluated: 1) the EI^{14,15} (frontal horn diameter divided by inner skull diameter obtained from the same transverse section); 2) degree of the CA^{16,17} (the angle between the lateral ventricles in the coronal plane measured through the posterior commissure perpendicular to the anterior–posterior commissure plane); 3) the narrowing of the superior parietal sulci (the narrowing of sulci at high convexity and medial parafalcine measured on the coronal plane; 0=normal, 1=narrowing of sulci restricted in the para-

falcine, and 2=narrowing extended to the vertex);¹⁸ and 4) the height of the Sylvian fissure (in millimeter; the height of the Sylvian fissure was measured in five coronal planes starting from the coronal view where the midbrain began to emerge based on the method described by Virhammar et al.¹⁹). The average value of the five different locations on both sides was recorded.^{19,20} Moreover, 5) the width of the temporal horn (in millimeter; the average of the maximal width of the right and left temporal horns on the transverse plane was used);¹⁹ 6) the severity of the perihippocampal fissure (PHF) dilatation (the dilatation of the PHF was subjectively measured on the transverse

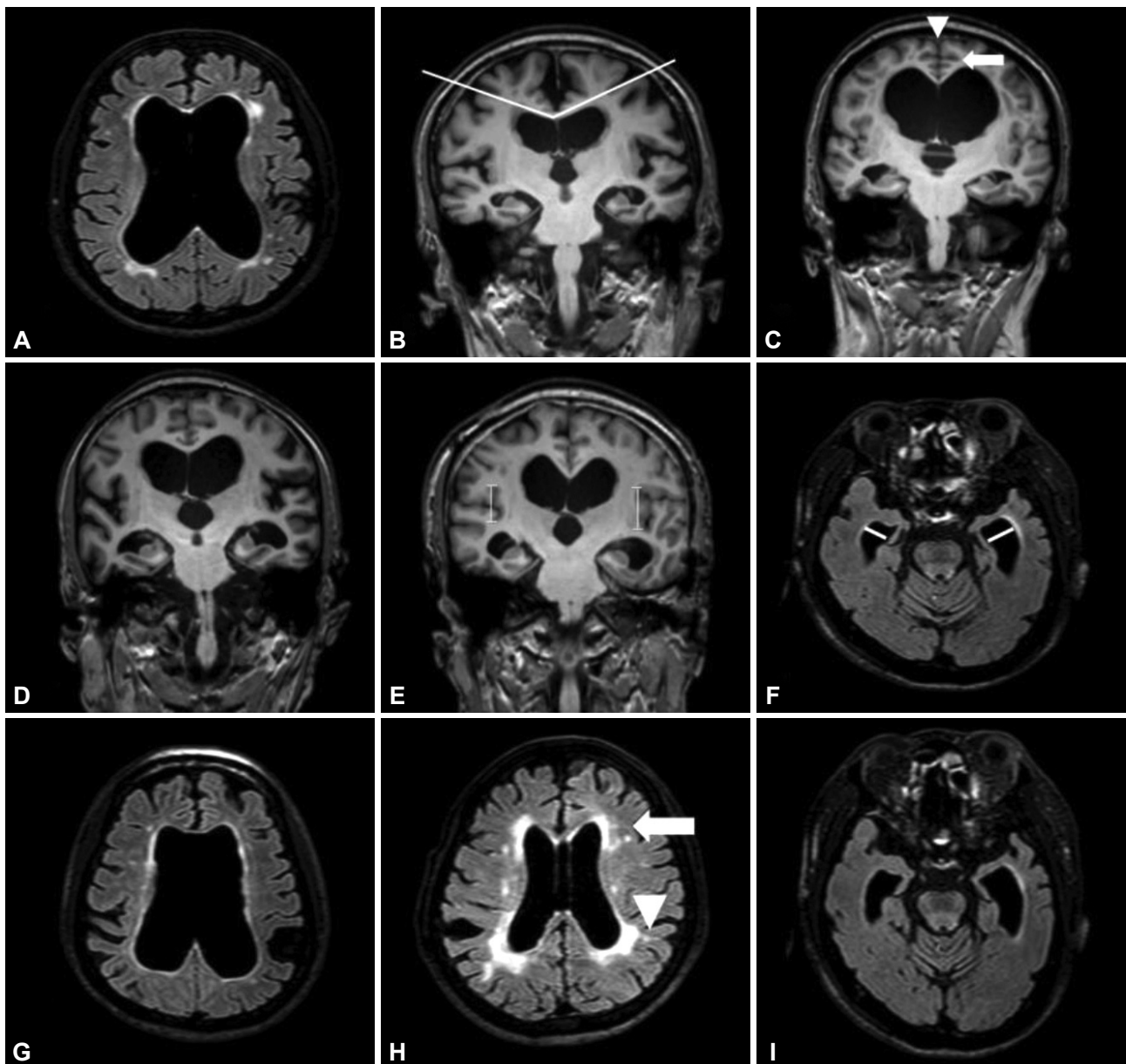


Figure 1. MRI parameters. A: EI. B: Degrees of the callosal angle. C: Narrowing of the superior parietal sulci, graded as 2=vertex. D: Height of the Sylvian fissure. E: Width of the temporal horn. F: Perihippocampal fissure dilatation, graded as 2=severe. G: Focally enlarged cerebral sulci, graded as 1=present. H: Periventricular hyperintensities, graded as 3=confluent areas. I: MTA scale, graded as 2.

and coronal planes; 0=none to mild, 1=moderate, and 2=severe);²¹ 7) the presence of focally enlarged cerebral sulci (the CSF accumulation in focally enlarged cerebral sulcus was graded as 0=not present and 1=present);^{22,23} 8) the severity of periventricular hyperintensities (Fazekas scale; 1=caps or pencil-thin lining, 2=smooth halo, and 3=irregular large symmetric hyperintensities extending out into the deep white matter region);²⁴ and 9) Scheltens' scale for medial temporal lobe atrophy (MTA scale; 0=no atrophy, 1=widening of choroid fissure only, 2=widening of choroid fissure and temporal horn of lateral ventricle, 3=moderate loss of hippocampal volume (decrease in height), and 4=severe hippocampal volume loss)²⁵ were also measured. Furthermore, the average of the left and right values was used for all measurements.²⁶

Statistical data analysis

For normally distributed continuous variables, univariate generalized linear model statistical analyses were employed for the between-group comparisons, including age and global CDR as covariates. Logistic regression was used when the normal distribution was not satisfied, including age and global CDR as covariates. Consequently, the cutoff values of continuous variables were determined using the receiver operating characteristic (ROC) curve. All hypotheses tests were two-sided. Bi-

nary logistic analyses were performed to get composite score. Statistical tests were conducted using Statistical Package for the Social Sciences, version 24 (IBM Corp., Armonk, NY, USA). The threshold of significance was set at $p < 0.05$ at both sides.

RESULTS

Participants

Table 1 presents demographic data for the 54 patients. The mean age (SD) at the time of MRI was 72.32 (8.69) and 81.41 (4.81) years in the iNPH and hydrocephalus ex vacuo groups, respectively. In addition, the difference in age between the two groups was statistically significant ($p < 0.001$). The global CDR showed the significant difference between the two groups ($p < 0.005$), 0.66 (0.28), and 1.00 (0.52), respectively. However, the other demographic data did not show a significant difference between the two groups.

Differences of radiological parameters in each group

The degree of the CA was smaller in the iNPH group than in the AD group, showing 87.35 ± 20.05 and 110.94 ± 16.66 in the iNPH and AD groups, respectively. The CA ($p < 0.05$) and height of the Sylvian fissure ($p < 0.05$) showed statistically significant differences between the two groups (Table 2). Furthermore, 80% and 31% of the patients in the iNPH and hydrocephalus ex vacuo groups had normal PHF dilation, respectively without statistical significance difference. However, Evans' Index was higher in iNPH group than Hydrocephalus ex vacuo group, 0.38 (0.05) vs. 0.35 (0.29), respectively, without statistical significance. Evans' index and width of temporal horn were greater in iNPH group than AD group, however, in this study without statistical significance. Absence of superior parietal sulci narrowing was found in more patients with AD than patients with iNPH with statistically significant difference ($p < 0.05$) (Table 3).

ROC analysis and binary logistic regression analysis

An ROC analysis was conducted to establish a diagnostic cutoff value for each of the above three variables, which displayed

Table 1. Demographic and cognitive characteristics of participants

	Idiopathic normal pressure hydrocephalus (N=25)	Hydrocephalus ex vacuo (N=29)	P
Age, years	72.32 (8.69) [†]	81.41 (4.81) [†]	<0.001
Sex, male, N (%) [*]	17 (68)	21 (72.4)	0.72
Education, years	9.76 (4.22) [†]	9.55 (6.16) [†]	0.88
Global CDR	0.66 (0.28) [†]	1.00 (0.52) [†]	0.005
MMSE	20.60 (5.13) [†]	18.34 (5.49) [†]	0.13

^{*}a Mann-Whitney U-test or a chi-squared test was used for comparisons, [†]mean (standard deviation). CDR: clinical dementia rating scale, MMSE: Mini-Mental State Exam

Table 2. Comparison of continuous radiological parameters between the idiopathic Normal Pressure Hydrocephalus and Hydrocephalus ex vacuo group

Continuous variables	Idiopathic normal pressure hydrocephalus (N=25)	Hydrocephalus ex vacuo (N=29)	p [*]	F	Partial Eta squared
Evans' index	0.38 (0.05) [†]	0.35 (0.29) [†]	0.07	3.50	0.07
Degrees of callosal angle (°)	87.36 (20.05) [†]	110.94 (16.66) [†]	0.01	6.99	0.12
Height of Sylvian fissure (mm)	27.19 (3.02) [†]	25.41(3.04) [†]	0.01	8.69	0.15
Width of temporal horn (mm)	9.01 (2.44) [†]	8.34 (2.35) [†]	0.51	0.45	0.01

^{*}univariate generalized linear model analyses were conducted for the between-group comparisons, including age and clinical dementia rating scale as covariates, [†]mean (standard deviation)

statistically significant differences between the two groups (Figure 2). When maximizing sensitivity and specificity, the cut-off values were as follows: CA, 89.8; height of the Sylvian fissure, 26.2; and narrowing of superior parietal sulci, 0/1. Based

on these values, iNPH could be differentiated from hydrocephalus ex vacuo with a sensitivity of 0.90, 0.64, and 0.68, respectively, and specificity of 0.64, 0.76, and 0.83, respectively. The area under the curve (AUC) was 0.81, 0.65, and 0.79, respectively.

Table 3. Comparison of categorical radiological parameters between the idiopathic Normal Pressure Hydrocephalus and Hydrocephalus ex vacuo group

Categorical variables	Idiopathic normal pressure hydrocephalus (N=25)	Hydrocephalus ex vacuo (N=29)	OR†
Superior parietal sulci narrowing			
Normal	8 (32)	24 (82.8)	0.07*
Narrowing of sulci restricted in the parafalcine	4 (16)	4 (13.8)	0.15
Narrowing extended to the vertex	13 (52)	1 (3.4)	1
Perihippocampal fissure dilatation			
None to mild	20 (80)	9 (31)	5.50
Moderate	2 (8)	10 (34.5)	1.07
Severe	3 (12)	10 (34.5)	1
Focally enlarged cerebral sulci			
Not present	17 (68)	26 (89.7)	0.22
Present	8 (32)	3 (10.3)	1
Periventricular hyperintensities			
Caps or pencil-thin lining	0 (0)	6 (20.7)	8.5e-10
Smooth halo	12 (48)	8 (27.6)	1.31
Irregular large symmetric hyperintensities extending out into the deep white matter region	13 (52)	15 (51.7)	1
Medial temporal atrophy scale			
	Left/right	Left/right	5.69‡
No atrophy	1 (4)/1 (4)	0 (0)/0 (0)	
Only widening of choroid fissure	3 (12)/3 (12)	0 (0)/0 (0)	
Also widening of temporal horn of lateral ventricle	5 (20)/5 (20)	5 (17.2)/7 (24.1)	
Moderate loss of hippocampal volume (decrease in height)	11 (44)/12 (48)	14 (48.3)/12 (41.4)	2.20
Severe volume loss of hippocampus	5 (20)/4 (16)	10 (34.5)/10 (34.5)	1

* $p < 0.05$, †logistic regression was conducted, including age and CDR as covariates, ‡OR for groups of no atrophy, only widening of choroid fissure, and also widening of temporal horn of lateral ventricle in medial temporal atrophy scale, which were grouped as one category due to small numbers for logistic statistical analysis. CDR: clinical dementia rating scale, OR: odds ratios

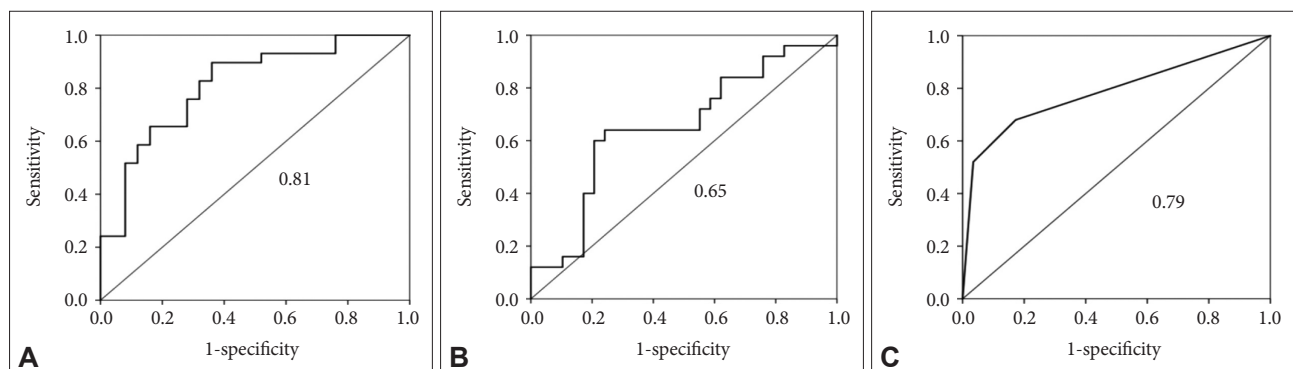


Figure 2. ROC curve to differentiate iNPH from hydrocephalus ex vacuo. A: Degrees of the callosal angle. B: Height of the Sylvian fissure. C: Narrowing of superior parietal sulci. The AUC is shown. ROC: receiver operating curve, AUC: area under the curve, iNPH: idiopathic normal pressure hydrocephalus.

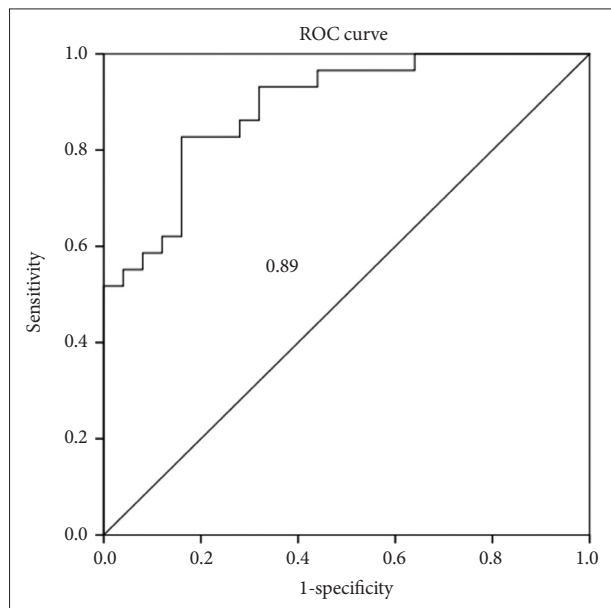


Figure 3. ROC of the composite score to differentiate iNPH from hydrocephalus ex vacuo. ROC analysis of this composite score showed an AUC of 0.89. ROC: receiver operating curve, AUC: area under the curve, iNPH: idiopathic normal pressure hydrocephalus.

The binary logistic regression model was used to identify radiological parameters from the aforementioned three meaningful variables, which optimally differentiated patients with iNPH from patients with hydrocephalus ex vacuo to investigate if the combination of these three factors is more useful in distinguishing iNPH from AD than each element. The final model included the absence of narrowing of superior parietal sulci [$\exp(b)=0.296$, $p=0.024$], narrow degree of the CA [$\exp(b)=1.056$, $p=0.041$], and height of the Sylvian fissure [$\exp(b)=0.745$, $p=0.029$]. Including these three variables into the model classified iNPH and hydrocephalus ex vacuo with an accuracy of 0.78. The rate of the explained variance according to Nagelkerke's estimate for R^2 ²⁷ was 0.58. Binary logistic regression yielded a composite score defined as $0.055 \times CA - 0.294 \times \text{height of the Sylvian fissure} - 1.218 \times \text{narrowing of superior parietal sulci} + 3.186$. ROC analysis of this composite score showed an AUC, sensitivity, and specificity of 0.89, 0.83, and 0.84, respectively (Figure 3).

DISCUSSION

This study aims to evaluate and compare the radiological parameters of brain MRI between subjects with iNPH and AD patients with hydrocephalus ex vacuo. When comparing the radiological parameters, the degree of callosal angle (CA), the height of the Sylvian fissure and narrowing of superior parietal sulci, which are statistically significant variables, would be useful for comparing the two groups (Figure 4).

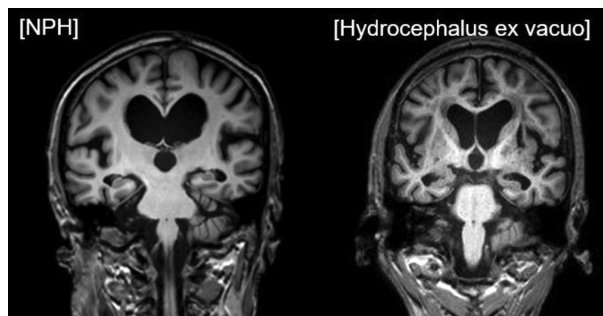


Figure 4. MRI images of the idiopathic normal pressure hydrocephalus and hydrocephalus ex vacuo. The image on the left represents iNPH, showing a small callosal angle (CA), dilatation of the Sylvian fissure, and narrowing of superior parietal sulci. The image on the right represents hydrocephalus ex vacuo with a large CA, no dilatation of the Sylvian fissure, and absence of narrowing of superior parietal sulci. iNPH: idiopathic normal pressure hydrocephalus.

The degree of the CA was smaller in the iNPH group than in the AD group, showing 87.35 ± 20.05 and 110.94 ± 16.66 in the iNPH and AD groups, respectively. This result was similar to the findings of other previous studies. In a study by Ishii et al.,¹⁷ the CA in the iNPH group (mean \pm SD, 66 ± 14) was significantly smaller than that in the AD group (104 ± 15), and the cutoff value was 90. Unlike the AD, iNPH fills the ventricles with the CSF pressure on the upper part of the brain, causing small CA, which may indicate ventriculomegaly. In contrast, diffuse brain atrophy such as in AD causes wider CA. However, the widening of the temporal horn cannot differentiate iNPH from hydrocephalus ex vacuo. Regarding the lack of differences in the width of the temporal horn between the iNPH and AD groups in this study, the temporal lobe atrophy may result in the widening of the temporal horn similar to iNPH.

Evans' Index could be used as the radiological parameter of iNPH since the ventricular enlargement may not be entirely attributable to cerebral atrophy as AD although it has high sensitivity but low specificity for iNPH. In this study, Evans' Index showed no statistical significant difference between the two groups. Absence of narrowing of superior parietal sulci (grade 0=normal) was statistically significant after controlling age and global CDR (Table 3). Due to diffuse brain atrophy such as AD, absence of narrowing of superior parietal sulci would manifest in AD. Unlike AD, iNPH could show the narrowing of superior parietal sulci as the ventriculomegaly progresses.

The height of the Sylvian fissure in this study showed the difference between the two groups. The combination of the Sylvian fissure widening and the narrowing at the vertex has been termed disproportionately enlarged subarachnoid space hydrocephalus (DESH), reflecting the disproportionality of the CSF between the superior and inferior CSF spaces,¹⁰ which would be the typical sign of iNPH. Among the signs of DESH, the widening of the inferior CSF, such as the Sylvian fissure widening,

may differentiate iNPH from hydrocephalus ex vacuo. In the temporal lobe, the typical sign of iNPH may be the dilatation of the temporal horn due to CSF increase. However, in this study, the width of the temporal horn was not statistically different between the two groups. The PHF is not dilated in iNPH and is sometimes compressed because no communication exists between the temporal horn and the PHF through the choroid plexus.²⁸ But, the dilatation of the PHF was not statistically different between hydrocephalus ex vacuo and NPH.

No differences exist between the two groups in the presence of focally enlarged cerebral sulci and the severity of periventricular hyperintensities. White matter changes, including periventricular and deep white matter hyperintensity, are common in patients with iNPH and AD. Barber et al.²⁹ accentuated that periventricular hyperintensities displayed positive correlations with age and were prominent not only in vascular dementia but also in AD. According to a previous study, periventricular white matter hyperintensities correspond to the loss, demyelination, and gliosis of ependymal lining induced by ventricular enlargement,³⁰ prompting abnormal hydrodynamic changes in the CSF and an increase in the water content of the white matter.³¹⁻³³ The induction of compensatory CSF flow into the periventricular white matter region via the pathological disruption of the ependyma is similar, although the mechanisms of ventricular enlargement may differ between iNPH and AD. This similarity explains the presence of periventricular white matter hyperintensities in both patients with AD and iNPH when examined through MRI.

Kitagaki et al.²⁰ reported the presence of a few sulci dilations that allows distinguishing between patients with AD and iNPH. However, the severity of focally enlarged cerebral sulci parameters in the present study did not show any statistically significant differences between patients with AD with ventriculomegaly and patients with iNPH ($p=0.20$). This may be because focally dilated sulci are not a common feature in iNPH. In this study, only 32% of patients with iNPH had focally dilated sulci; this is similar to a study by Hashimoto et al.,³⁴ which reported 29%. This suggests that focally dilated sulci are not reliable imaging markers for iNPH diagnosis.

Since the diagnosis of iNPH is complicated by the variability existing in its clinical presentation and course, both clinical findings and radiological parameters would be much more helpful for the correct diagnosis of iNPH. The radiological parameters hold the significance as the noninvasive technique to distinguish various diseases such as AD. The composite scores generated from the logistic regression results of the degree of the CA, the height of the Sylvian fissure and narrowing of superior parietal sulci, which are statistically significant variables, would be useful for comparing the two groups (AUC, 0.89).

This study has several limitations. First, problems in gener-

alizing the results of this study exist because the subjects were retrospectively recruited at one hospital. Second, the diagnosis of iNPH and AD relied upon clinical diagnostic criteria. The use of amyloid PET would have provided a more accurate diagnosis for patients with hydrocephalus ex vacuo, although the diagnostic uncertainty between the NPH and AD was excluded. Third, due to lack of technological support, the computer analyses in the brain MRI imaging was not used. In addition, the power of the study may be low because of the small overall sample size. Thus, a larger study is needed in the future.

The findings of this study suggest that narrowing of the CA, dilatation of the Sylvian fissure and narrowing of superior parietal sulci may be used as reliable radiological markers to differentiate patients with iNPH from those with hydrocephalus ex vacuo. The composite score using narrowing of the CA, dilatation of the Sylvian fissure and narrowing of superior parietal sulci in the brain MRI, combined with clinical findings would be helpful in distinguishing iNPH with AD.

Availability of data and materials

The datasets used and/or analyzed during the current study are available from the corresponding author on reasonable request.

Acknowledgments

Supported by grant no. 26-2014-42 from the SK Telecom Research Fund.

Conflicts of Interest

The authors have no potential conflicts of interest to disclose.

Author Contributions

Conceptualization: Sun-Won Park, Jun-Young Lee, Jee-Young Lee, Hwancheol Son, Yu Kyeong Kim, Sang Hyung Lee. Data curation: Minkyung Kim, Sun-Won Park, Hongrae Kim, Jung Hyo Rhim. Formal analysis: Minkyung Kim, Sun-Won Park, Hongrae Kim, Jung Hyo Rhim. Funding acquisition: Sang Hyung Lee. Methodology: Sun-Won Park, Jun-Young Lee, Soowon Park, Sang Hyung Lee. Writing—original draft: Minkyung Kim, Hongrae Kim, Jun-Young Lee. Writing—review & editing: Minkyung Kim, Sun-Won Park, Jun-Young Lee, Jung Hyo Rhim, Soowon Park, Jee-Young Lee, Hwancheol Son, Yu Kyeong Kim, Sang Hyung Lee.

ORCID iDs

Minkyung Kim	https://orcid.org/0000-0001-6282-5612
Sun-Won Park	https://orcid.org/0000-0002-5063-2685
Jun-Young Lee	https://orcid.org/0000-0002-5893-3124
Hongrae Kim	https://orcid.org/0000-0002-9319-7521
Jung Hyo Rhim	https://orcid.org/0000-0001-5822-9770
Soowon Park	https://orcid.org/0000-0002-3348-940X
Jee-Young Lee	https://orcid.org/0000-0002-9120-2075
Hwancheol Son	https://orcid.org/0000-0001-5033-0153
Yu Kyeong Kim	https://orcid.org/0000-0002-3282-822X
Sang Hyung Lee	https://orcid.org/0000-0003-4720-955X

REFERENCES

1. Relkin N, Marmarou A, Klinge P, Bergsneider M, Black PM. Diagnosing idiopathic normal-pressure hydrocephalus. *Neurosurgery* 2005;57

- (3 Suppl):S4-S16; discussion ii-v.
2. Ryska P, Slezak O, Eklund A, Malm J, Salzer J, Zizka J. Radiological markers of idiopathic normal pressure hydrocephalus: relative comparison of their diagnostic performance. *J Neurol Sci* 2020;408:116581.
 3. Hebb AO, Cusimano MD. Idiopathic normal pressure hydrocephalus: a systematic review of diagnosis and outcome. *Neurosurgery* 2001;49:1166-1184.
 4. Yasar S, Jusue-Torres I, Lu J, Robison J, Patel MA, Crain B, et al. Alzheimer's disease pathology and shunt surgery outcome in normal pressure hydrocephalus. *PLoS One* 2017;12:e0182288.
 5. Marmarou A, Bergsneider M, Klinge P, Relkin N, Black PM. The value of supplemental prognostic tests for the preoperative assessment of idiopathic normal-pressure hydrocephalus. *Neurosurgery* 2005;57(3 Suppl):S17-S28; discussion ii-v.
 6. Martin-Laez R, Caballero-Arzapalo H, Valle-San Roman N, Lopez-Menendez LA, Arango-Lasprilla JC, Vazquez-Barquero A. Incidence of idiopathic normal-pressure hydrocephalus in Northern Spain. *World Neurosurg* 2016;87:298-310.
 7. Miskin N, Patel H, Franceschi AM, Ades-Aron B, Le A, Damadian BE, et al. Diagnosis of normal-pressure hydrocephalus: use of traditional measures in the era of volumetric MR imaging. *Radiology* 2017;285:197-205.
 8. Di Ieva A, Valli M, Cusimano MD. Distinguishing Alzheimer's disease from normal pressure hydrocephalus: a search for MRI biomarkers. *J Alzheimers Dis* 2014;38:331-350.
 9. Tarnaris A, Kitchen ND, Watkins LD. Noninvasive biomarkers in normal pressure hydrocephalus: evidence for the role of neuroimaging. *J Neurosurg* 2009;110:837-851.
 10. Graff-Radford NR, Jones DT. Normal pressure hydrocephalus. *Continuum (Minneapolis)* 2019;25:165-186.
 11. Ambarki K, Israelsson H, Wahlin A, Birgander R, Eklund A, Malm J. Brain ventricular size in healthy elderly: comparison between Evans index and volume measurement. *Neurosurgery* 2010;67:94-99; discussion 99.
 12. Kojoukhova M, Koivisto AM, Korhonen R, Remes AM, Vanninen R, Soininen H, et al. Feasibility of radiological markers in idiopathic normal pressure hydrocephalus. *Acta Neurochir (Wien)* 2015;157:1709-1718; discussion 1719.
 13. McKhann G, Drachman D, Folstein M, Katzman R, Price D, Stadlan EM. Clinical diagnosis of Alzheimer's disease: report of the NINCDS-ADRDA Work Group under the auspices of Department of Health and Human Services Task Force on Alzheimer's Disease. *Neurology* 1984;34:939-944.
 14. Evans WA. An encephalographic ratio for estimating ventricular enlargement and cerebral atrophy. *Arch Neurol Psychiatry* 1942;47:931-937.
 15. Toma AK, Holl E, Kitchen ND, Watkins LD. Evans' index revisited: the need for an alternative in normal pressure hydrocephalus. *Neurosurgery* 2011;68:939-944.
 16. Virhammar J, Laurell K, Cesarini KG, Larsson EM. The callosal angle measured on MRI as a predictor of outcome in idiopathic normal-pressure hydrocephalus. *J Neurosurg* 2014;120:178-184.
 17. Ishii K, Kanda T, Harada A, Miyamoto N, Kawaguchi T, Shimada K, et al. Clinical impact of the callosal angle in the diagnosis of idiopathic normal pressure hydrocephalus. *Eur Radiol* 2008;18:2678-2683.
 18. Sasaki M, Honda S, Yuasa T, Iwamura A, Shibata E, Ohba H. Narrow CSF space at high convexity and high midline areas in idiopathic normal pressure hydrocephalus detected by axial and coronal MRI. *Neuroradiology* 2008;50:117-122.
 19. Virhammar J, Laurell K, Cesarini KG, Larsson EM. Preoperative prognostic value of MRI findings in 108 patients with idiopathic normal pressure hydrocephalus. *AJNR Am J Neuroradiol* 2014;35:2311-2318.
 20. Kitagaki H, Mori E, Ishii K, Yamaji S, Hirono N, Imamura T. CSF spaces in idiopathic normal pressure hydrocephalus: morphology and volumetry. *AJNR Am J Neuroradiol* 1998;19:1277-1284.
 21. Holodny AI, Waxman R, George AE, Rusinek H, Kalnin AJ, de Leon M. MR differential diagnosis of normal-pressure hydrocephalus and Alzheimer disease: significance of perihippocampal fissures. *AJNR Am J Neuroradiol* 1998;19:813-819.
 22. Holodny AI, George AE, de Leon MJ, Golomb J, Kalnin AJ, Cooper PR. Focal dilation and paradoxical collapse of cortical fissures and sulci in patients with normal-pressure hydrocephalus. *J Neurosurg* 1998;89:742-747.
 23. Wikkelso C, Andersson H, Blomstrand C, Matousek M, Svendsen P. Computed tomography of the brain in the diagnosis of and prognosis in normal pressure hydrocephalus. *Neuroradiology* 1989;31:160-165.
 24. Fazekas F, Chawluk JB, Alavi A, Hurtig HI, Zimmerman RA. MR signal abnormalities at 1.5 T in Alzheimer's dementia and normal aging. *AJR Am J Roentgenol* 1987;149:351-356.
 25. Scheltens P, Launer LJ, Barkhof F, Weinstein HC, van Gool WA. Visual assessment of medial temporal lobe atrophy on magnetic resonance imaging: interobserver reliability. *J Neurol* 1995;242:557-560.
 26. Rhemtulla M, Brosseau-Liard PE, Savalei V. When can categorical variables be treated as continuous? A comparison of robust continuous and categorical SEM estimation methods under suboptimal conditions. *Psychol Methods* 2012;17:354-373.
 27. Nagelkerke NJD. A note on a general definition of the coefficient of determination. *Biometrika* 1991;78:691-692.
 28. Holodny AI, George AE, Golomb J, de Leon MJ, Kalnin AJ. The perihippocampal fissures: normal anatomy and disease states. *Radiographics* 1998;18:653-665.
 29. Barber R, Scheltens P, Gholkar A, Ballard C, McKeith I, Ince P, et al. White matter lesions on magnetic resonance imaging in dementia with Lewy bodies, Alzheimer's disease, vascular dementia, and normal aging. *J Neurol Neurosurg Psychiatry* 1999;67:66-72.
 30. Akai K, Uchigasaki S, Tanaka A, Komatsu A. Normal pressure hydrocephalus. Neuropathological study. *Acta Pathol Jpn* 1987;37:97-110.
 31. Chimowitz MI, Estes ML, Furlan AJ, Awad IA. Further observations on the pathology of subcortical lesions identified on magnetic resonance imaging. *Arch Neurol* 1992;49:747-752.
 32. Fazekas F, Kleinert R, Offenbacher H, Schmidt R, Kleinert G, Payer F, et al. Pathologic correlates of incidental MRI white matter signal hyperintensities. *Neurology* 1993;43:1683-1689.
 33. Zimmerman RD, Fleming CA, Lee BC, Saint-Louis LA, Deck MD. Periventricular hyperintensity as seen by magnetic resonance: prevalence and significance. *AJR Am J Roentgenol* 1986;146:443-450.
 34. Hashimoto M, Ishikawa M, Mori E, Kuwana N. Diagnosis of idiopathic normal pressure hydrocephalus is supported by MRI-based scheme: a prospective cohort study. *Cerebrospinal Fluid Res* 2010;7:18.